THE JOURNAL OF BIOLOGICAL CHEMISTRY VOL. 287, NO. 28, pp. 23698–23709, July 6, 2012

Threonine-120 Phosphorylation Regulated by Phosphoinositide-3-Kinase/Akt and Mammalian Target of Rapamycin Pathway Signaling Limits the Antitumor Activity of Mammalian Sterile 20-Like Kinase 1*[S]

Received for publication, March 6, 2012, and in revised form, May 21, 2012 Published, JBC Papers in Press, May 22, 2012, DOI 10.1074/jbc.M112.358713

Filiz Kisaayak Collak[‡§], Kader Yagiz[‡§], Daniel J. Luthringer[¶], Bahriye Erkaya[‡§], and Bekir Cinar[‡§1]

From the [‡]Department of Medicine and Biomedical Sciences, Samuel Oschin Comprehensive Cancer Institute, Los Angeles, California 90048, the [§]Department of Medicine, David Geffen School of Medicine, University of California at Los Angeles, Los Angeles, California 90095 , and the [¶]Department of Pathology and Laboratory Medicine, Cedars-Sinai Medical Center, Los Angeles, California 90048

Background: The molecular mechanisms that regulate the hippo-like Mst1 protein kinase remain elusive.
Results: PI3-kinase and mTOR signaling regulate Mst1 phosphorylation in a discrete cell location.
Conclusion: Phospho-Thr-120 restricts Mst1 functions, leading cancer cell growth and survival.
Significance: Mst/Hippo signaling is a promising drug target in human cancers.

Mst1/Stk4, a hippo-like serine-threonine kinase, is implicated in many cancers, including prostate cancer. However, the mechanisms regulating Mst1 remain obscure. Here, we characterized the effects of phospho-Thr-120 on Mst1 in prostate cancer cells. We demonstrated that phospho-Thr-120 did not alter the nuclear localization or cleavage of Mst1 in a LNCaP or castration-resistant C4-2 prostate tumor cell model, as revealed by a mutagenesis approach. Phospho-Thr-120 appeared to be specific to cancer cells and predominantly localized in the nucleus. In contrast, phospho-Thr-183, a critical regulator of Mst1 cell death, was exclusively found in the cytoplasm. As assessed by immunohistochemistry, a similar distribution of phospho-Mst1-Thr-120/Thr-183 was also observed in a prostate cancer specimen. In addition, the blockade of PI3K signaling by a small molecule inhibitor, LY294002, increased cytoplasmic phospho-Mst1-Thr-183 without having a significant effect on nuclear phospho-Mst1-Thr-120. However, the attenuation of mammalian target of rapamycin (mTOR) activity by a selective pharmacologic inhibitor, Ku0063794 or CCI-779, caused the up-regulation of nuclear phospho-Mst1-Thr-120 without affecting cytoplasmic phospho-Mst1-Thr-183. This suggests that PI3K and mTOR pathway signaling differentially regulate phospho-Mst1-Thr-120/Thr-183. Moreover, mutagenesis and RNAi data revealed that phospho-Thr-120 resulted in C4-2 cell resistance to mTOR inhibition and reduced the Mst1 suppression of cell growth and androgen receptor-driven gene expression. Collectively, these findings indicate that phospho-Thr-120 leads to the loss of Mst1 functions, supporting cancer cell growth and survival.

Mst1 (also known as Stk4), related to hippo (*hpo*) in *Drosophila*, is a multifunctional serine/threonine kinase (1). Mst1 has three paralogs (Mst2, Mst3, and Mst4), and Mst1 is the prototype of this family (1). Mst1 consists of a conserved amino (NH_2)-terminal (NT) catalytic domain and carboxyl (COOH)-terminal (CT) regulatory domain (2) with the inclusion of nuclear export and nuclear localization signals, as well as inhibitory and dimerization functions (3). Posttranslational modification by phosphorylation appears to play an important role in regulating Mst1. Several phosphorylation sites, presumably at the threonine residue, have been identified in the Mst1 structure, and they have been shown to negatively or positively regulate Mst1 activity (4–6). Originally, Mst1 was identified as a proapoptotic protein activated during apoptosis (3). Mst1 phosphorylation at the Thr-183 residue in the activation loop and/or cleavage, leading to a catalytically more active nuclear Mst1-N form, are important molecular events for Mst1 activation and cell death function in mammalian cells (7–9).

In addition to its role in cell death, increasing lines of evidence suggests that Mst1, along with its closest paralog, Mst2 (Mst1/2), plays a fundamental role in the promotion of multiple cancers. For instance, the loss of Mst1/2 expression has been suggested in head and neck squamous cell carcinoma (10), soft tissue sarcoma (11), glioblastoma (12), and colorectal cancers (13), along with a poorer prognosis. Also, an altered subcellular distribution of Mst1 full-length (Mst1-FL)[2] with the loss of cytoplasmic expression and nuclear accumulation has been implicated in late-stage or advanced colorectal cancer (13). Moreover, evidence on the basis of genetic studies from multiple laboratories suggested that a liver-specific deletion of both

* This work was supported by an Edwin Beer Fellowship Award from the New York Academy of Medicine (to B. C.) and a Jesse and Donna Garber Foundation and Cedars-Sinai Medical Center Fellowship Award (to B. C.).
[S] This article contains supplemental Fig. 1 and Experimental Procedures.
[1] To whom correspondence should be addressed: Department of Medicine and Biomedical Sciences, Cedars-Sinai Medical Center; 8750 Beverly Blvd. Atrium 103, Los Angeles, CA 90048. Tel.: 310-423-8658; Fax: 310-423-8543; E-mail: bekir.cinar@cshs.org.

[2] The abbreviations used are: FL, full-length; AR, androgen receptor; mTOR, mammalian target of rapamycin; IP, immunoprecipitation; MTS, 3-(4,5-dimethylthiazol-2yl)-5-(3-carboxymethoxyphenyl)-2-(4-sulfophenyl)-2H-tetrazolium; DMSO, dimethyl sulfoxide; Dox, doxycycline; PrEC, primary prostate epithelial; ARE, androgen responsive element enhancer; PSA, prostate specific antigen; IF, Immunofluorescence; IHC, immunohistochemistry; WB, Western blot; Luc, luciferase.

Mst1/2 alleles in mice resulted in liver enlargement, hepatocellular carcinoma, and resistance to cell death inducers (14–16). Mst1/2 loss has also been shown to promote stem/progenitor cell expansion in mouse liver and intestine (14, 17).

Although the direct physiological significance of Mst1 in prostate tumorigenesis is yet to be established, a previous study from our laboratory demonstrated for the first time that the reduction or loss of Mst1 function might have a critical role in prostate cancer progression (18). In that study, we showed that Mst1 protein was progressively reduced during prostate cancer progression toward the castration-resistant, metastatic state in humans (18). Consistent with this observation, our recent study demonstrated that a gain of Mst1 function suppressed prostate cancer cell growth *ex vivo* and tumor growth in mice (19). In those studies, we identified Mst1 as a binding partner and negative regulator of androgen receptor (AR) and Akt1/protein kinase B (hereafter Akt) signaling (18, 19), which is central to prostate cancer cell survival and tumor progression. Nevertheless, other researchers suggest that the activation of PI3-kinase and Akt signaling by growth factors such as insulin-like growth factor could negatively regulate Mst1 in other cancer cell types (6, 12, 20). Despite these findings, the molecular mechanisms elucidating the regulation of Mst1 in prostate cancer cells remain elusive.

In this study, we investigated the significance of phospho-Thr-120 on Mst1 regulation in prostate cancer cells. The results showed that phospho-Thr-120 did not significantly alter the nuclear localization and cleavage of Mst1. Phospho-Mst1-Thr-120 was predominantly accumulated in the nucleus, whereas phospho-Thr-183, a positive regulator of Mst1 cell death, exclusively localized in the cytoplasm. PI3-kinase and mTOR signaling differentially regulated phospho-Mst1-Thr-120/Thr-183 in a discreet cell location. Phospho-Thr-120 significantly decreased the Mst1 suppression of cell growth, chemoresistance, and AR target genes expression. Taken together, these findings suggest that phospho-Thr-120 serves as a negative regulator of the Mst1 functions, which may have important therapeutic and prognostic implications in human cancers.

EXPERIMENTAL PROCEDURES

Plasmid Constructions, Antibodies, and Reagents—Construction of Myc-tagged Mst1 or the tetracycline/doxycycline-inducible HA-tagged Mst1 plasmid was described previously (19). The expression of each protein was under the control of the CMV promoter. Phosphorylation-deficient Thr-120A or Thr-387A or a phosphomimetic Thr-120D point mutation on HA-tagged or Myc-tagged Mst1-WT was generated using a QuikChange site-directed mutagenesis kit (Stratagene, La Jolla, CA). Double-stranded oligonucleotide surrounding a Thr-120 phosphorylation site amino acid residue was ligated into the BamH1 and EcoRI sites in pGEX-2TK vector to generate GST-Mst1-Thr-120 fusion. DNA sequencing and enzyme digestion were conducted to verify the orientation and fidelity of all vector constructs. A site-specific phospho-Mst1-Thr-120 antibody was custom-made using Mst1 peptide surrounding phospho-Thr-120 as an antigen (GenScript, Inc., Piscataway, NJ). Other antibodies and reagents used in this study are listed in the supplemental information.

Cell Fractionations and Protein Analysis—A nuclear extraction kit was used according to the protocol of the manufacturer (Affymetrix, Santa Clara, CA) to isolate cytoplasmic and nuclear fractions. Total cell lysates were prepared on ice-cold lysis buffer (20 mM HEPES (pH 7.4), 150 mM NaCl, 0.5% Nonidet P-40, 1 mM EDTA, protease inhibitors, and phosphatase inhibitors). Bacterially expressed GST peptides were purified by affinity chromatography on glutathione-Sepharose beads (GE Healthcare, Piscataway, NJ) and stored in PBS at 4 °C until use. Preactivated recombinant Akt1 kinase was obtained from Millipore (Billerica, MA). Protein concentrations were determined by the Lowry method (Bio-Rad). For immunoprecipitation (IP), cleared lysates were incubated with a protein-specific antibody overnight at 4 °C. Antibody-antigen complexes were collected using protein A- or G-Sepharose (GE Healthcare) and washed three times with lysis buffer to remove unbound proteins. The precipitates were resolved by SDS-PAGE, transferred to nitrocellulose membranes, and blocked either with PBST or TBST (0.1% Tween 20) containing 5% (w/v) skim milk powder. Signals were detected using SuperSignal West Pico chemiluminescence substrate (Thermo Scientific, Roxford, IL).

Cell-based and Animal Experiments—Cell viability was measured using CellTiter 96 AQueous with 3-(4,5-dimethylthiazol-2-yl)-5-(3-carboxymethoxyphenyl)-2-(4-sulfophenyl)-2H-tetrazolium (MTS) reagent according to the instructions of the manufacturer (Promega, Madison, WI). Briefly, cells in RPMI culture medium plus 10% fetal bovine serum were added to 96-well plates at 4×10^3 cells/well in quadruplicate. Parental C4-2 cells were incubated with Ku0063794, CCI-779, or BEZ 235 up to 72 h post-cell seeding. At 24 h post-Mst1-WT or point mutant Mst1-Thr-120A induction or siRNA transfection, cells were treated with DMSO control, CCI-779, or rapamycin and incubated for up to 72 h. MTS and phenazine methosulfate solution (20 μl/well) was added, and the absorbance at 490 nm was recorded using a microplate reader (BMG Labtech, Cary, NC). For the clonogenic assay, 500 cells/well in 6-well plates were seeded and cultured for a week in the presence of doxycycline (Dox, 0.5 μg/ml) in serum-fed conditions. The medium was changed every 3 days. Colonies were fixed with formaldehyde (4% v/v) and stained with crystal violet (0.5%). Representative views from triplicate experiments were photographed and quantified. For the soft agar colony formation assay, 5×10^3 cells were suspended in 1 ml of 0.3% agarose with Dox (0.5 μg/ml) and overlaid onto 1 ml of 0.5% solidified bottom agarose/well in 6-well plates. After solidification, the top agarose was covered with 1 ml of RPMI with 10% FBS and Dox (0.5 μg/ml). The culture medium was changed every 3 days. After 14 days, colonies were photographed and quantified. For the sphere-forming assay in Matrigel, 80 μl Matrigel was added per well in 8-well chamber slides. After 30 min, 500–1000 cells/well were suspended in 400 μl of ice-cold 10% Matrigel in phenol red-free RPMI medium. Cells were overlaid with 200 μl of RPMI with 10% FBS and Dox (0.5 μg/ml) and grown for 10–14 days with a change of medium every 3 days. Spheres were photographed and quantified manually. Animal experiments were conducted as described previously (19) and according to the protocol approved by the Institutional Animal Care and Use Committee. Briefly, 2×10^6 C4-2/Vector, C4-2/HA-Mst1, or

C4-2/HA-Mst1-Thr-120A cells mixed with Matrigel (1:1 ratio) in a 100-μl volume were injected subcutaneously into nude male mice. Mice were then treated with Dox (0.5 mg/ml) in drinking water to induce Mst1 expression 1 day after cell inoculation. Tumor growth was monitored for 6 weeks with weekly tumor size measurements.

Cell Transfections and Reporter Assays—Prostate cancer cell lines LNCaP, C4-2, or C4-2B4 were cultured in T-medium with 5% FBS (Gemini Bio Products, West Sacramento, CA) or in RPMI 1640 with 10% FBS. Primary prostate epithelial cells (PrEC) were grown in PrEBM medium (Lonza). PC3M, HEK-293, HeLA, MCF-7, and OVCAR5 cells were cultured in high-glucose DMEM (Invitrogen) with 10% FBS. Cell culture mediums were supplemented with 1% penicillin and streptomycin. Cells were incubated at 37 °C supplemented with 5% CO_2. siRNA specific to Mst1, Mst2, or scrambled (control) siRNA was from Thermo Scientific/Dharmacon RNAi Technologies (Roxford, IL). Double-stranded siRNA oligonucleotides were transfected using Dharma*FECT-2* transfection reagent (Thermo Scientific). Plasmids were transfected using Lipofectamine 2000 reagent as described (19) and according to the instructions of the manufacturer (Invitrogen). Luciferase reporter gene activity was determined using a luciferase assay system (Promega) and a bioluminescence microplate reader (BMG Labtech) according to the instructions of the manufacturer and as described (19). Relative light units were normalized to total protein, and the data were presented as luciferase activity. The tetracycline/doxycycline-inducible C4-2 cell model with stable HA-tagged Mst1-Thr-120A expression was established as described previously (19).

ChIP Assay—A ChIP assay was performed as described previously (19). Briefly, C4-2 cells were transiently transfected with vector, Mst1-WT, or Mst1-Thr-120 mutant. Cells grown in serum-starved conditions were treated with R1881 (10 nM) or EtOH (vehicle) for 6 h. DNA enriched with anti-AR antibody was quantified by semiquantitative PCR using primer sets surrounding the AREIII region within the androgen-responsive element (ARE) enhancer core of the prostate-specific antigen (PSA) promoter (21).

Cell Imaging and Microscopy—For immunofluorescence (IF), cells were seeded on sterile 8-well chamber slides at 70% confluence and fixed in 3% paraformaldehyde for 30 min at room temperature for blocking and for antibody labeling. Probes included Alexa Fluor 488 conjugated with secondary goat anti-rabbit antibody (1:500). Cell nuclei were detected by DAPI staining (Vector Laboratory, Burlingame, CA). Cells were imaged at ×20 magnification by fluorescence microscopy (Nikon Eclipse *Ti* model). Immunohistochemistry (IHC) was performed on 5-micron-thick paraffin sections. Tissue slides were deparaffinized and rehydrated using standard techniques. Antigen retrievals were achieved by 5 min of pressure-cooking and then cooling down to room temperature for 1 h. Blocking was performed by double endogenous enzyme block in 10 min. Tissues were incubated with primary antibodies (phospho-Mst1-Thr-120 and phospho-Mst1-Thr-183) at 4 °C overnight. They were subjected to DakoCytomation EnVision plus horseradish peroxidase reagent for 30 min. Signals were detected by adding substrate hydrogen peroxide using diaminobenzidine as a chromogen and counterstained by hematoxylin. Slides were then dehydrated and mounted. All reagents were obtained from Dako Corp. (Carpinteria, CA). All experiments involved in human subjects were conducted according to a protocol approved by the Institutional Review Board.

Statistical Analysis—Values are expressed as mean ± S.D. An unpaired Student's *t* test was conducted to analyze for differences between treatments. Statistical significance was set at $p \leq 0.05$.

RESULTS

Full-length Mst1 Is Accumulated in Prostate Cancer Cell Nuclei—Our studies and others have shown that Mst1 can exist in multiple forms as Mst1-FL and/or the caspase-cleaved Mst1-N or Mst1-C (8, 18). Nuclear accumulation of Mst1, especially the cleaved Mst1-N, has been suggested as a prominent mediator of cell death (8). Nevertheless, our previous studies indicated that Mst1 was abundantly found in the nucleus, yet cells were morphologically perfectly normal (18, 19). In this study, we primarily used the LNCaP prostate cancer cell model or its castration-resistant C4-2 subline. These cell models are ideal because they are AR-positive and possess the hyperactivation of PI3K and mTOR pathway signaling (23, 24). A non-cancerous PrEC cell model was also included as a control in this study. The first demonstration was to determine which Mst1 form (Mst1-FL or the cleaved Mst1-N) localized primarily to the nucleus. Cytoplasmic and nuclear fractions from PrEC, LNCaP, or C4-2 cells were isolated and the levels of Mst1-FL or the cleaved Mst1-N were assessed by Western blot analysis using the antibody raised against the amino terminal domain of Mst1. The results of this experiment showed that although the majority of Mst1-FL was found in the cytoplasm of normal PrEC cells, it was almost equally distributed between the cytoplasm and nuclei in LNCaP or C4-2 prostate cancer cells (Fig. 1*A*, *upper panel*). In addition, we assessed the levels of phospho-Thr-183 under the above experimental conditions by Western blot analysis. The results showed that phospho-Mst1-Thr-183 was exclusively detected in the cytoplasm, regardless of the transformation of the prostate epithelium (Fig. 1*A*, *center panel*). Very low or undetectable cleaved total or a phospho-Mst1-N (Thr-183) form was detected only in the cytoplasm by Western blot analysis under the same experimental conditions above.

To independently verify the above data, IP with amino-terminal Mst1 antibody and Western blot analysis with carboxy-terminal Mst1 antibody was performed (Fig. 1*B*). Using the same antibody set, nuclear localization of Mst1-FL was also determined by IF analysis in serum-fed and serum-starved conditions (Fig. 1, *C* and *D*). Results of these experiments showed that Mst1-FL was found in the nuclei. Serum deprivation did not significantly alter the nuclear localization of Mst1-FL. These findings are consistent and indicate that Mst1-FL, but not the cleaved Mst1-N form, localizes primarily to the nuclei.

Phospho-Thr-120 That Is Primarily Accumulated in the Nuclei Does Not Alter the Nuclear Localization and Cleavage of Mst1—Phosphorylation of Mst1 at Thr-120 was suggested to prevent the nuclear localization of the protein and cleavage in ovarian cancer cells (6). To test whether phospho-Thr-120

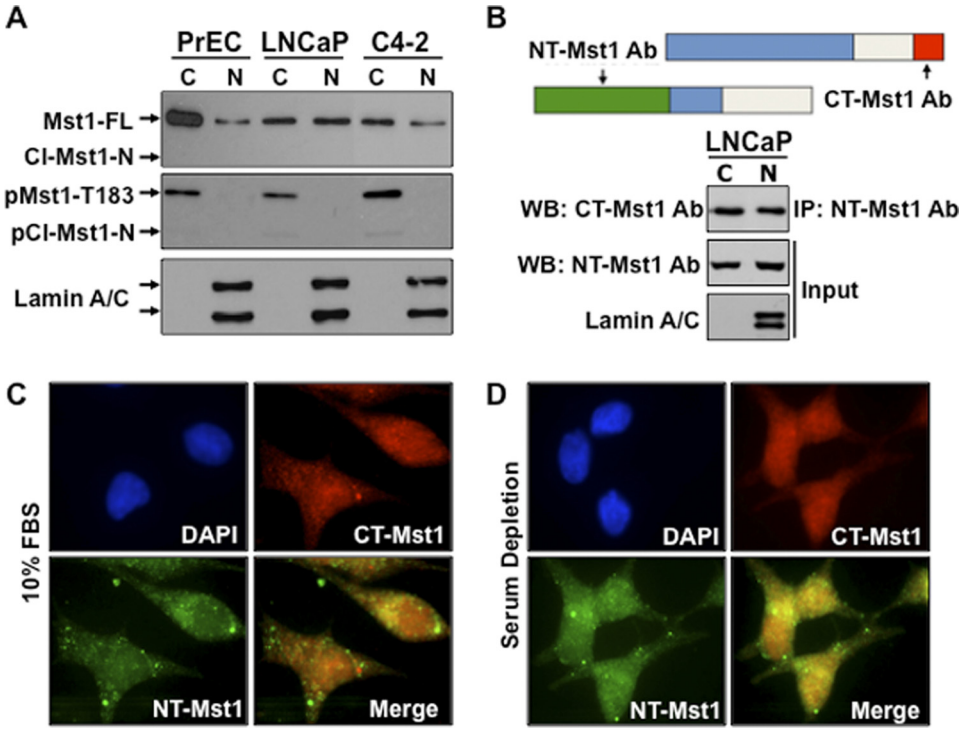

FIGURE 1. **The full-length Mst1, but not the cleaved-Mst1-N, localizes to the nuclei of prostate cancer cells.** *A*, endogenous total or phospho-Mst1 protein in cytoplasmic (*C*) and nuclear (*N*) fractions from hTERT-PrEC, LNCaP, and C4-2 cells. *Cl*, cleaved. *B*, coimmunoprecipitation and Western blot analysis of full-length endogenous Mst1 from cytoplasmic and nuclear fractions of LNCaP cells. The model is representation of the relative locations of NH_2-terminal (*NT*) or COOH-terminal (*CT*) Mst1 antibody. Lamin A/C was used as a nuclear fraction control. Co-IP and WB analysis were performed with corresponding antibodies. *C* and *D*, IF images of endogenous Mst1 protein in LNCaP cells grown in serum in *C*, 10% FBS, or without serum in *D*. The Mst1 protein was visualized using Mst1-NT (rabbit polyclonal) as a primary and FITC-labeled as a secondary antibody (*green*) or Mst1-CT (mouse polyclonal) as a primary and Cy3-labeled as a secondary antibody (*red*). DAPI-stained cell nuclei (*blue*). Data are representative of multiple experiments.

would show similar behaviors on the Mst1 in prostate cancer cells, we generated a phosphorylation-deficient Mst1-Thr-120A mutant. Mst1-WT or the Mst1-Thr-120A mutant was transiently expressed in C4-2 cells from which nuclear and cytoplasmic fractions were isolated. Western blot analysis showed that the Thr-to-Ala mutation (Thr-120A) did not affect Mst1 nuclear localization and cleavage in comparison to Mst1-WT (Fig. 2*A*). Similarly, the induction of Mst1-Thr-120A mutant in HeLA cells did not alter Mst1 cleavage, leading about 36-kDa Mst1-N, compared with the Mst1-WT (supplemental Fig. 1*A*).

To examine the levels of native phospho-Mst1-Thr-120 in prostate cancer cells, we generated a custom-designed and site-specific rabbit polyclonal antibody. The antibody was developed using the chemically synthesized and Thr-120-phosphorylated peptide corresponding to the NH_2 terminus of human Mst1 surrounding the Thr-120 residue. As demonstrated by IP/WB analysis, ectopically expressed Mst1-Thr-120A mutant did not react with the phospho-Thr-120 antibody compared with the Mst1-WT (supplemental Fig. 1*B*). This suggests that the antibody was specific to phospho-Mst-Thr-120. In addition, Fig. 2*B* shows that the antibody recognized the native phospho-Mst-Thr-120 protein from LNCaP and C4-2 cells, as assessed by Western blot analysis in total cell lysates.

To further verify the antibody specificity and examine the subcellular localization of phospho-Mst1-Thr-120, we conducted an RNAi experiment. LNCaP cells were transiently transfected with the pool of Mst1 gene-specific or scramble (mock) siRNA. The levels of phospho-Mst1-Thr-120 were assessed by Western blot analysis in cytoplasmic and nuclear fractions obtained from LNCaP cells with or without Mst1 knockdown. The results demonstrated that phospho-Mst-Thr-120 was accumulated predominantly in the nucleus under this experimental condition because Mst1 knockdown reduced the antibody reactivity to low or undetectable levels (Fig. 2*C* and supplemental Fig. 1*C*). To further confirm the above data, we then performed an IP experiment with phospho-Mst1-Thr-120 antibody and a Western blot analysis with total Mst1 antibody. Phospho-Mst1-Thr-120 was indeed localized primarily in cell nuclei (Fig. 2*D*).

As a complementary approach, the analysis of phospho-Mst1-Thr-120 by IF in LNCaP and C4-2 cells using phospho-Thr-120 peptide antibody were performed. The results, consistent with the biochemical data, demonstrated that phospho-Mst1-Thr-120 primarily localized in the nuclei (Fig. 2*E*). Serum starvation did not significantly alter nuclear phospho-Mst1-Thr-120 (supplemental Fig. 1*D*). As assessed by Western blot analysis, a similar distribution of phospho-Mst1-Thr-120 was also observed in C4-2B4, a bone metastatic subline of C4-2 cells, and in bone metastatic PC3M cells (supplemental Fig. 1*E*).

To evaluate the clinical relevance of our *ex vivo* findings, we conducted an IHC analysis of phospho-Mst1-Thr-120 in normal prostate and prostate tumor tissue samples. The results showed that the levels of phospho-Mst1-Thr-120 in the nuclei were increased dramatically in cancerous prostate compared with the non-cancerous counterparts (Fig. 2*F*, *left panels*). In

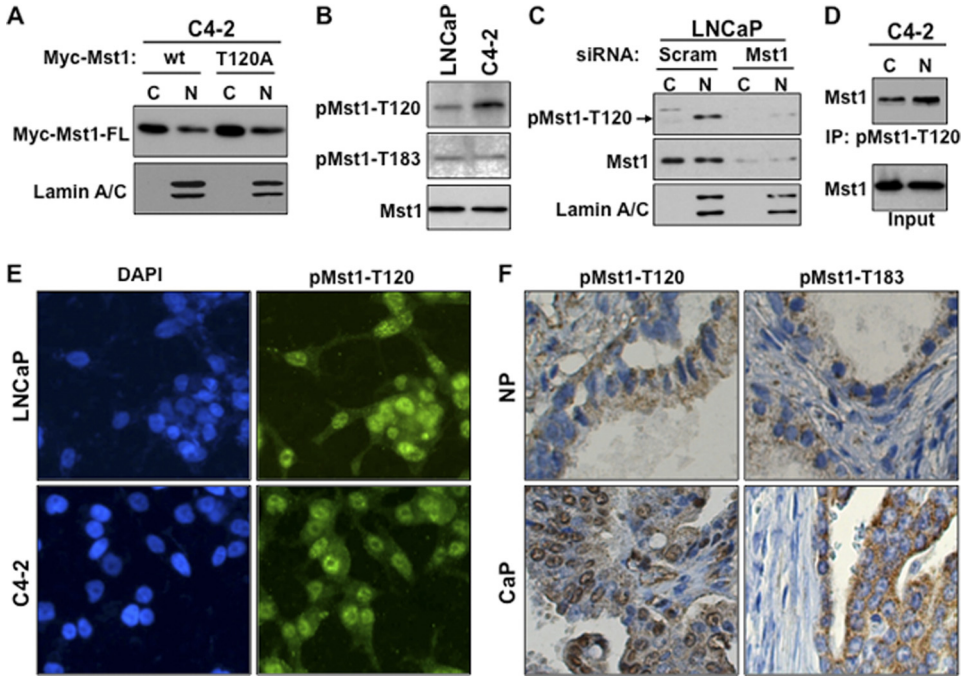

FIGURE 2. **Phospho-Thr-120 does not alter Mst1 nuclear localization and cleavage in prostate cancer cells.** *A*, WB analysis of ectopically expressed Mst1-WT and Mst1-Thr-120 protein in cytoplasmic (*C*) and nuclear (*N*) fractions from C4-2 cells. Cells were transiently transfected with a Myc-tagged Mst1-WT and Mst1-Thr-120 plasmid. *B*, analysis of the total and phospho-Mst1-Thr-120 or -Thr-183 in total lysates of LNCaP or C4-2 cells by Western blot analysis. *C*, RNAi knockdown experiment. Cells were transfected with scramble or Mst1-specific siRNA, and levels of total or pMst1-Thr-120 were analyzed in cytoplasmic and nuclear fractions. 15 μg of total protein/lane was resolved by SDS-PAGE. *D*, IP with pMst1-Thr-120 antibody. Phospho-Mst1-Thr-120 protein was precipitated from nuclear and cytoplasmic fractions, respectively. 1 mg of total protein was used in the IP, and Western blot analyses were performed with antibody to the total Mst1 protein. *E*, IF staining of pMst1-Thr-120 in LNCaP and C4-2 PCa cells. Alexa Fluor 488-stained (*green*) pMst1-Thr-120 protein and DAPI-stained (*blue*) the nuclei (magnification $\times$20). *F*, IHC analysis of clinical samples from non-cancerous or normal prostate ($n = 5$) and cancerous prostate tissues ($n = 15$); magnification $\times$20. IHC was performed using pMst1–120 and pMst1-Thr-183 antibodies. Images are representative of multiple staining. *NP*, normal prostate; *CaP*, carcinoma of the prostate. Data are representative of multiple experiments.

addition, the analysis of phospho-Mst1-Thr-183 by IHC in clinical samples revealed that although the majority of phospho-Mst1-Thr-120 was found in the nucleus, the phospho-Mst1-Thr-183 protein was exclusively detected in the cytoplasm, albeit with increased levels in cancerous prostate compared with the non-cancerous counterparts (Fig. 2*E*, *right panels*).

The PI3K and mTOR Pathways Differentially Regulate Phospho-Mst1-Thr-120/Thr-183—A report suggested that PI3K/Akt signaling could regulate phospho-Mst1-Thr-120, which, in turn, was implicated to negatively affect Mst1 phosphorylation at Thr-183 in ovarian cancer cells (6). As outlined in Fig. 3*A*, we generated GST-Mst1-WT or GST-Mst1-Thr-120A mutant fusion peptide and performed non-radioactive kinase assays using preactivated, recombinant Akt as a kinase. The data in Fig. 3*B* showed that the Akt kinase phosphorylated recombinant GST-Mst1-Thr-120 peptide *ex vivo*. The phosphorylation was specific because the kinase assay with GST-only or GST-Mst1-Thr-120A mutant peptide displayed an undetectable or very low signal, respectively, compared with the GST-Mst1-WT. Consistent with this observation, the treatment of LNCaP cells with the PI3K inhibitor, LY294002, prevented phospho-Mst1-Thr-120, as assessed by Western blot analysis in total cell lysates (Fig. 3*C*). In addition, this experiment showed that although LY294002 treatment completely inhibited phospho-Akt-Ser-473, the treatment failed to completely eliminate phospho-Akt-Thr-308 under the same experimental conditions (Fig. 3*C*).

To determine whether the inhibition of PI3K/Akt signaling alters nuclear phospho-Mst1-Thr-120 or cytoplasmic phospho-Mst1-Thr-183, LNCaP or C4-2 cells were treated with DMSO vehicle (-) or LY294002 (+) in serum-starved conditions. The levels of phospho-Mst1-Thr-120/Thr-183 were analyzed by Western blot analysis in the cytoplasmic and nuclear fractions isolated from LNCaP or C4-2 cells under the above conditions. The results showed that LY294002 did not significantly alter nuclear phospho-Mst1-Thr-120 compared with the vehicle control (Fig. 3, *D* (*lane 4 versus lane 2*) and *E* (*lane 4 versus lane 2*), respectively). However, LY294002 increased phospho-Mst1-Thr-183 in the cytoplasm of LNCaP (Fig. 3*D*, *lane 3 versus lane 1*) or C4-2 cells (*E*, *lane 3 versus lane 1*).

The mTOR serine-threonine kinase is an important mediator or regulator of PI3K/Akt signaling (25). The mTOR kinase exists in a rapamycin-sensitive mTOR complex 1 (mTORC1) and a rapamycin-insensitive mTOR complex 2 (mTORC2) (26). To assess whether the inhibition of mTOR signaling by a selective pharmacological inhibitor alters phospho-Mst1-Thr-120/Thr-183, LNCaP or C4-2 cells were treated with Ku0063794, a potent inhibitor of mTORC1/C2. C4-2 cells were also treated with CCI-779, a potent mTORC1 inhibitor in addition to the Ku0063794. Ku0063794 did not alter nuclear phospho-Mst1-Thr-120 levels in LNCaP cell nuclei (Fig. 3*D*, *lane 6 versus lane 2*), whereas Ku0063794 or CCI-779 increased phospho-Mst1-Thr-120 levels in C4-2 cell nuclei (Fig. 3*E*, *lane 6* or *lane 8 versus lane 2*, respectively) relative to vehicle (DMSO)

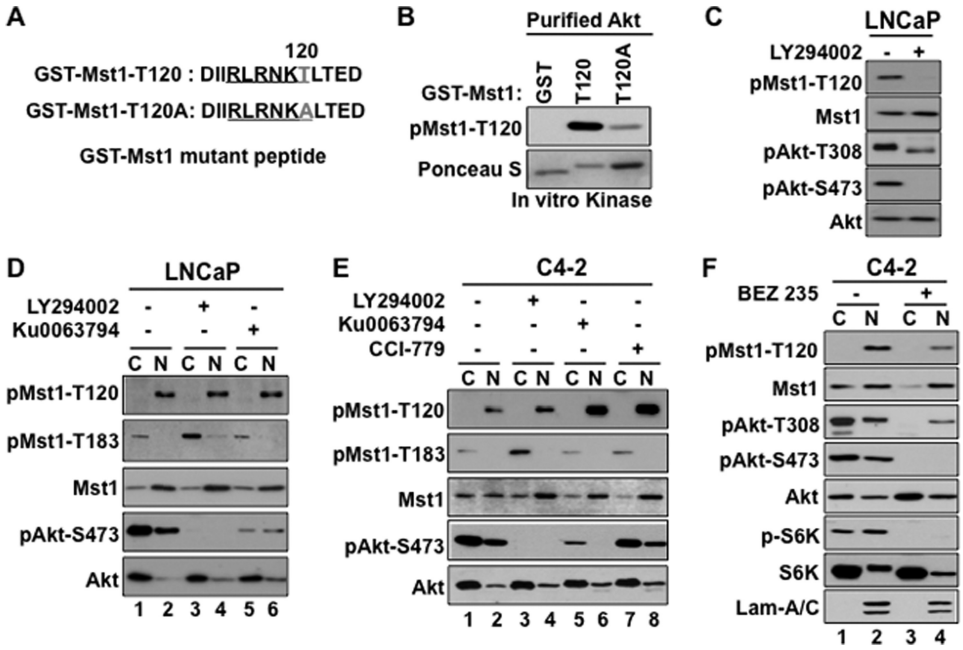

FIGURE 3. **Phospho-Mst1-Thr-120 is a downstream target of the PI3K and mTOR pathway signaling.** *A*, schematic representation of the GST-Mst1 peptide with WT Thr-120 or T120A mutations. *B*, *in vitro* kinase assay with bacterially expressed and purified GST-only, GST-Mst1, or the GST-Mst1-T120A mutant peptide and the recombinant preactivated Akt kinase. Western blot analyses were probed with pMst1-Thr-120 antibody. Ponceau S-stained purified GST, GST-Mst1-Thr-120, or the GST-Mst1-T120A mutant peptide. *C*, analysis of phospho-Mst1-Thr-120 levels by Western blotting in total cell lysate. LNCaP cells were treated with DMSO (vehicle) or a specific PI3K inhibitor, LY294002 (20 μM). *D* and *E*, analysis of phospho-Mst1-Thr-120 levels by Western blotting in the cytoplasm and nuclear fractions. LNCaP cells were treated with DMSO (vehicle), LY294002 (20 μM), or mTOR inhibitor Ku0063794 (1 μM) in serum-starved conditions, and C4-2 cells (*E*) were treated with mTORC1 inhibitor and CCI-779 (1 μM) in addition to LY294002 or Ku0063794 under the same experimental conditions as in *D*. 15 μg of total protein per lane were resolved by SDS-PAGE. *E*, C4-2 cells treated with DMSO or dual PI3K and mTOR inhibitor BEZ 235 (0.5 μM). DMSO control or drug treatment in *C*, *D*, *E*, or *F* was performed under serum-deprived conditions. Western blot analyses were probed with antibodies to corresponding proteins at 3 h post-treatment. *Lam-A/C*, Lamin-A/C. Data are representative of multiple experiments.

treatment. The Western blot analysis of phospho-Mst1-Thr-183 under the same conditions above revealed that as opposed to the LY294002, Ku0063794 or CCI-779 treatment did not alter phospho-Mst1-Thr-183 levels in the cytoplasm (Fig. 3, *D* and *E*). Taken together, signals initiated from or mediated by the PI3K and mTOR pathways differentially regulate phospho-Mst1-Thr-120/Thr-183, albeit in a distinct cell location.

Pharmacological inhibition of mTOR was reported to activate PI3K/Akt by a negative feedback mechanism (27, 28). To test whether the activation of PI3K/Akt signaling has a role in the up-regulation of nuclear phosho-Mst1-Thr-120 in response to the mTOR inhibitor, C4-2 cells were treated with DMSO or BEZ 235, a dual pharmacologic inhibitor of PI3K and mTOR. The data from the Western blot analysis showed that a combinatorial inhibition of PI3K and mTOR by BEZ 235 reduced nuclear phospho-Mst1-Thr-120 compared with the control (Fig. 3*F*, *lane 4 versus lane 2*) or single agent (Fig. 3*E*, *lane 8 versus lane 2*). A similar result was also obtained in C4-2 cells treated with LY294002 plus Ku0063794 or LY294002 plus CCI-779 (data not shown). These findings suggest that PI3K/Akt signaling plays a significant role in the nuclear up-regulation of phospho-Mst1-Thr-120 by mTOR inhibitors.

Phospho-Mst1-Thr-120 Is Associated with Resistance to mTOR Inhibition—To assess whether a functional link between the up-regulation of phospho-Mst1-Thr-120 and C4-2 cell resistance to the mTOR inhibitor, we performed a series of cell viability assays under various conditions. First, we showed that C4-2 cells displayed resistance to the Ku0063794 or CCI-779 mediation of reduced cell viability compared with the LNCaP parental line (Fig. 4*A*). Second, a concurrent inhibition of the PI3K and mTOR pathways by BEZ 235 significantly reduced C4-2 cell viability in a dose-dependent manner ($p < 0.027$) (Fig. 4*B*). In addition, we have shown that C4-2 cells were relatively resistance to the PI3K inhibitor, LY294002, compared with the LNCaP cells (not shown) (19). Third, the induction of phosphorylation-deficient Mst1-Thr-120A mutant significantly sensitized C4-2 cells to CCI-779 compared with the Mst1-WT ($p < 0.001$) (Fig. 4*C*). As a complementary approach, we also assessed the cell viability using phosphomimetic Mst1-T120D mutant along with Mst1-T120A. The results showed that C4-2 cells expressing the phosphomimetic Mst1-T120D mutant conferred resistance to CCI-779, as opposed to Mst1-T120A (Fig. 4*D*).

A genetic study suggested that Mst1 and Mst2 were functionally redundant in the mammalian system because Mst1 and Mst2 compensated for the absence of each other during development (29). In that study, Mst1 or Mst2 knockout mice did not show any apparent developmental defects, whereas both Mst1 and Mst2 (Mst1/2) knockouts were embryonic lethal. Therefore, we proposed that if Mst1 or Mst2 would compensate for the absence of the functions of each other, then CCI-779 could reduce the viability of C4-2 cells in Mst1 or Mst2, but not both Mst1/2, knockdown conditions compared with the scramble control. To test this, C4-2 cells were transiently transfected with scramble, Mst1, Mst2, or Mst1/2 siRNA followed by treatment with CCI-779 or DMSO vehicle. Under these conditions, cell viability was determined (Fig. 4*E*). In comparison to the scramble siRNA, CCI-779 reduced C4-2 cell viability by 40% in

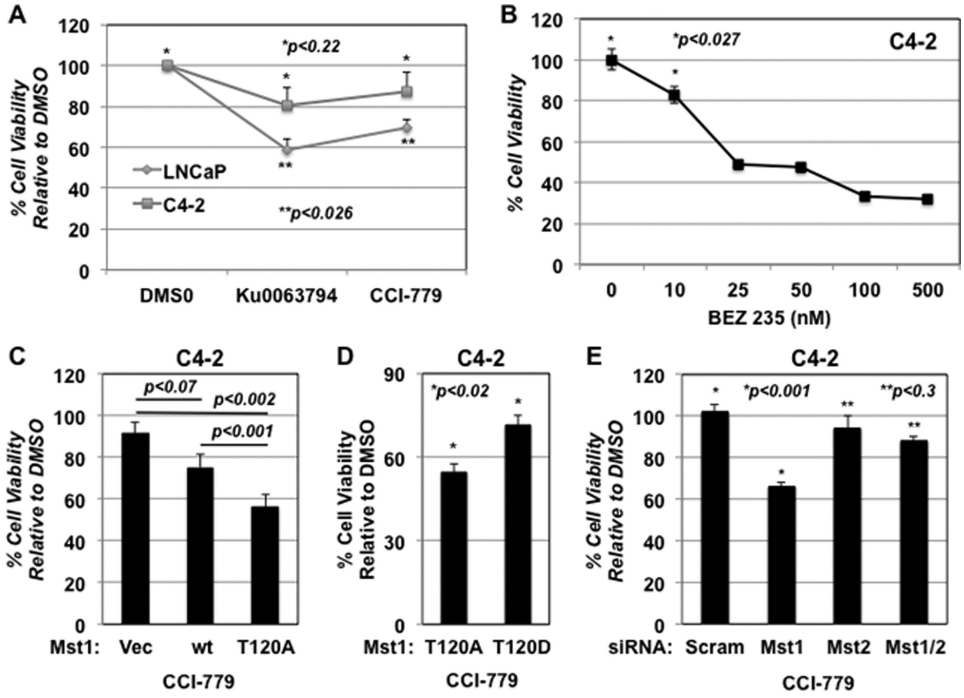

FIGURE 4. **Phopsho-Mst1-Thr-120 appears to be associated with C4-2 prostate tumor cell resistance to mTOR inhibitors.** *A*, LNCaP or C4-2 cells were treated with DMSO, Ku0063794 (1 μM), or rapamycin (1 μM). *B*, C4-2 cells were treated with increasing doses (0, 10, 25, 50, 100, and 500 nM) of the dual PI3K and mTOR inhibitor BEZ 235. Control or drug treatments were performed in T medium supplemented with 5% FBS and 1% penicillin/streptomycin. *C*, effects of CCI-779 (0.5 μM) on C4-2 cells engineered to express vector, Mst1-WT, or Mst1-Thr-120A mutant. *D*, effects of CCI-779 (0.5 μM) on C4-2 cells that were transiently transfected with phosphorylation-deficient Mst1-Thr-120A or phosphomimetic Mst1-T120D in a 96-well plate in triplicates, followed by CCI-779 treatment. 100 ng of plasmid DNA was used per well. An MTS assay (*A* 490 nm) at 48 h post-drug treatment was performed to determine cell viability in experiments *A*, *B*, *C*, and *D*. *E*, effects of DMSO or CCI-779 (0.5 μM) on C4-2 cell viability with scramble control, Mst1, Mst2, and Mst1/2 knockdown conditions. Gene-specific siRNA was used to knock down Mst1, Mst2, or Mst1/2 protein in a transient transfection assay. Cell viability was determined by MTS (*A* 490 nm) at 72 h post-transfection. Data are representative of multiple experiments.

the Mst1 knockdown condition, which was statistically significant ($p < 0.001$). However, C4-2 cells with Mst2 knockdown displayed resistance to CCI-779 (Fig. 4*E*). As expected, cells with Mst1/2 knockdown showed resistance to mTOR inhibition by CCI-779 (Fig. 4*E*). These findings support the notion that Mst1 might be functionally attenuated and thus failed to sensitize C4-2 cells to CCI-779. This experiment also revealed that Mst2 was functional and able to sensitize C4-2 cells to the CCI-779 in the absence of Mst1.

Phospho-Thr-120 Restrains the Ability of Mst1 to Suppress Cell Growth ex vivo and Tumor Growth in Mice—To assess whether phospho-Thr-120 has a negative impact on the Mst1 control of cell growth, we conducted a series of biological assays using the C4-2/Mst1-Thr-120A mutant along with C4-2/vector (negative control) or C4-2/Mst1-WT cells (positive control) (Fig. 5*A*). We first showed that the induction of the Mst1-T120A mutant significantly reduced C4-2 cell growth compared with the Mst1-WT in monolayer culture (Fig. 5*B* and supplemental Fig. 1*F*). Second, the induction of the Mst1-T120A mutant significantly reduced the clonogenic ability of C4-2 cells *in vitro* in comparison with the Mst1-WT ($p < 0.01$) or vector control ($p < 0.002$) (Fig. 5, *B* and *C*). Third, and most importantly, the induction of the Mst1-T120A mutant in C4-2 cells notably ($p < 0.02$) inhibited colony formation in soft agar (Fig. 5, *D* and *E*) and sphere formation in Matrigel (Fig. 6*A*) compared with the Mst1-WT.

To determine whether the Mst1-T120A mutant would also reduce the tumor-forming ability of C4-2 cells, we performed xenograft experiments in mice. Immunodeficient and nude male mice were subcutaneously inoculated with inducible C4-2/vector, C4-2/Mst1-WT, or C4-2/Mst1-T120A cells, and animals in all groups were then treated with Dox (0.5 mg/ml) in their drinking water for 6 weeks to induce Mst1 expression. Tumor sizes were measured manually every week starting from the second week post-inoculation. Induction of the Mst1-T120A mutant resulted in the formation of significantly ($p < 0.02$) smaller tumors in both number and size than the Mst1-WT or vector control (Fig. 6, *B* and *C*). These observations indicate that phospho-Thr-120 limits the antiproliferative and/or antitumor activity of Mst1.

Phospho-Thr-120 Diminishes the Ability of Mst1 to Attenuate AR-dependent Gene Expression—A previous study from our laboratory suggested that Mst1 antagonizes androgen-mediated AR-target gene expression through protein-protein interaction and by altering the AR-chromatin complexes (19). We used this finding to assess whether phospho-Thr-120 alters the Mst1 diminution of AR activity. To test this, we conducted luciferase (Luc) reporter assays using a PSA promoter linked to the Luc reporter (PSA-Luc) in LNCaP and C4-2 cells with or without androgen treatment. PSA is a well characterized AR-regulated gene in prostate cancer cells (30). Fig. 7, *A* and *B*, demonstrated that the induction of Mst1-T120A mutant displayed significantly superior inhibitory effects on androgen-induced AR-driven PSA promoter activation than the Mst1-WT ($p < 0.02$). In addition, the Thr-387 residue in Mst1 was reported as another phospho site for the Akt kinase, and the

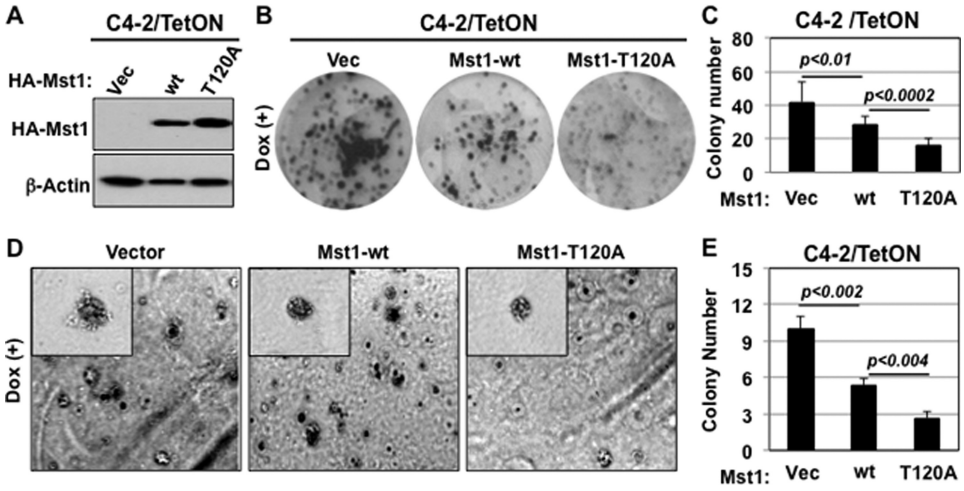

FIGURE 5. **Phospho-Thr-120 decreases the Mst1 suppression of clonogenesis in monolayer culture *ex vivo*.** *A*, the blot shows the analysis of ectopically expressed HA-tagged Mst1-WT or Mst1-Thr-120A mutant protein by Western blot analysis. Total protein was prepared from Tet-ON-C4-2/HA-Mst1-WT or -C4-2/HA-Mst1-T120A cells. C4-2/vector cells were used as a negative control. *B*, clonogenic ability of C42 cells expressing stable vector, Mst1-WT, or Mst1-Thr-120A under Dox (0.5 μg/ml) in culture. Colonies were fixed and visualized by crystal violet staining at 7 days post-Mst1-WT and Mst1-T120A mutant induction. *C*, the *graph* is the quantification of clones in *B*. *D*, colony formation of C4-2/vector, C4-2/Mst1-WT, or C4-2/Mst1-T120A cells in soft agar in the presence of Dox (0.5 μg/ml). *E*, the *graph* is the quantification of colonies formed in soft agar in *D*. Data are representative of multiple experiments.

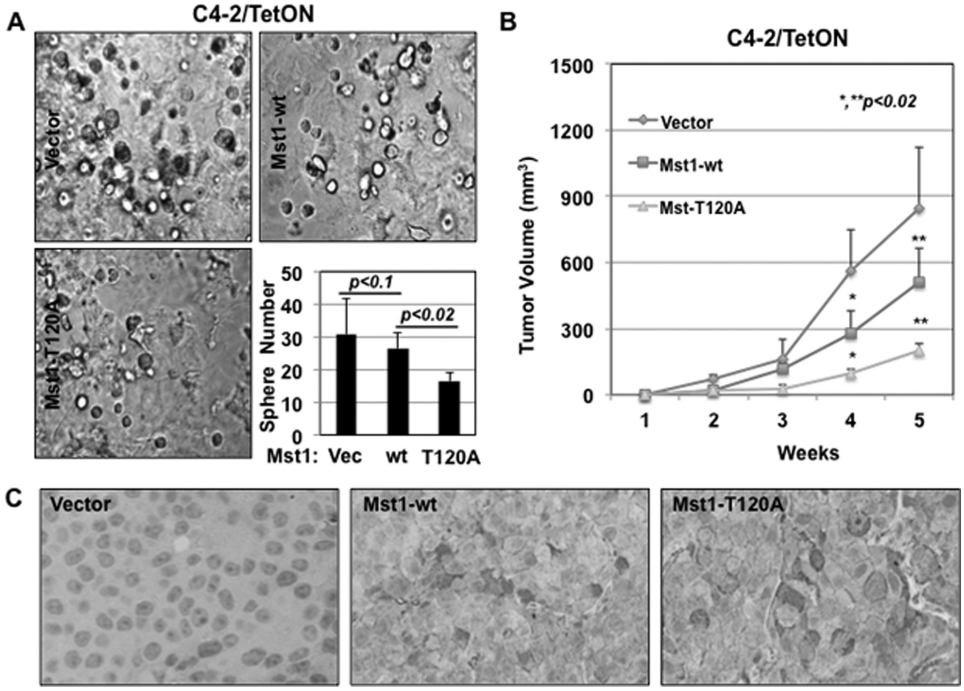

FIGURE 6. **Phospho-Thr-120 reduces the Mst1 diminution of sphere formation in Matrigel *ex vivo* and tumor formation in mice.** *A*, three-dimensional cell growth (sphere formation) in Matrigel. Equal numbers of C4-2/vector, Mst1-WT, or Mst1-T120A cells were seeded. The cells were grown for 10 days in the presence of Dox (0.5 μg/ml). The *graph* is the quantification of spheres. Engineered C4-2 cells in all experiments were grown in serum-fed conditions. Data are representative of multiple experiments. *B*, tumor formation in xenografts. C4-2/vector ($n = 10$), C4-2/HA-Mst1-WT ($n = 6$), or C4-2/HA-Mst1-T120A ($n = 3$) cells were subcutaneously inoculated into intact nude male mice (10 animals per group). Animals were treated with Dox (0.5 mg/ml) in drinking water for 6 weeks. Tumor sizes were measured weekly. Tumor volumes were presented as a function of time for each group. *C*, IHC analysis of HA-Mst1 expression in tumor xenografts. Tissue sections were stained with HA tag antibody. *Blue* stained the nuclei. Magnification was $\times$200. Images are representative of multiple experiments.

phosphorylation of this site was suggested to prevent the Mst1 cell death function (5). However, when we performed the promoter reporter assay with the Mst1-T387A mutant, we did not observe any significant alteration of AR-dependent PSA promoter activation by androgen in comparison to the Mst1-WT (data not shown).

To test whether the Mst1-T120A mutant forms an increased protein complex with endogenous AR, which displayed a greater inhibitory effect on AR transactivation than the Mst1-WT, C4-2 cells were transiently transfected with a vector, Mst1-WT, or the Mst-T120A mutant construct. As revealed by co-IP/WB analysis, a protein-protein interaction between endogenous AR and the ectopically expressed Mst1-T120A mutant was about 40% greater than the Mst1-WT (Fig. 7*C*). A similar binding pattern between the AR and Mst-T120A mutant was also observed in total cell lysates obtained from

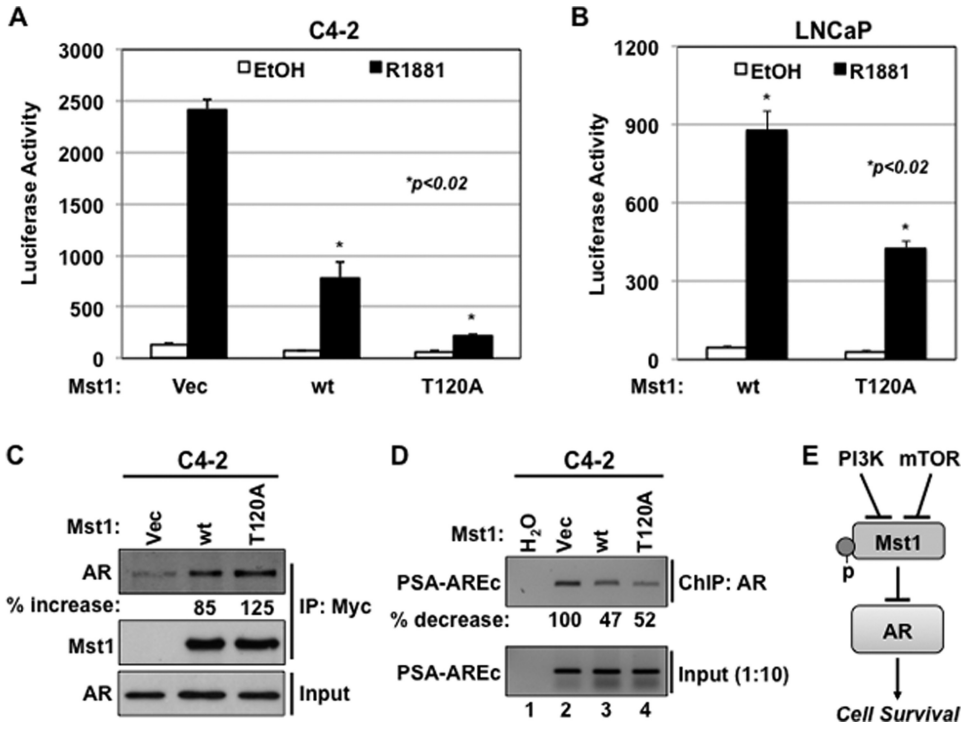

FIGURE 7. **Phospho-Thr-120 limits the Mst1 attenuation of androgen-mediated and AR-dependent gene expression.** *A* and *B*, PSA promoter reporter activity (p61-Luc) in C4-2 (*A*) and in LNCaP (*B*) cells that were transiently cotransfected with p61-Luc reporter and Vector, Mst1-WT, or the Mst1-T120A mutant construct followed by androgen induction in serum-starved conditions. Luciferase reporter assays were performed at 36 h post-transfection. The data normalized to the vector control were presented as luciferase activity. Data are represented as mean ± S.E. *C*, co-IP and WB analysis of Mst1 and endogenous AR interaction in C4-2 cells expressing transient Mock (*Vec*), Myc-Mst1-WT, or the Myc-Mst1-T120A mutant. Co-IP with anti-Myc antibody and WB analysis with an antibody to corresponding proteins was performed. The values of AR in the Myc-Mst1 immune complex were normalized to the Mst1 precipitant, and the data were expressed as percent (%) increase relative to vector control set to 0%. *D*, ChIP assay. C4-2 cells were transiently transfected with vector (*Vec*), Mst1-WT, or the Mst1-T12A mutant for 48 h. The ChIP assay was performed at 6 h after androgen (10 nM, R1881) treatment in serum-depleted conditions. Semiquantitative PCR was performed using a primer set covering the androgen response element core (*AREc*) region of the PSA promoter. The values of bond DNA were normalized to the input and expressed as percent (%) reduction. Data are representative of multiple experiments. *E*, model summarizes the conclusion of this study. *P*, phosphorylation.

AR-negative HEK-293 cells, in which AR and vector, Mst1-WT, or Mst-T120A were transiently coexpressed (data not shown).

To determine whether the Mst1-Thr-120 mutant alters the AR-chromatin complex formation that is also regulated by Mst1-WT, we performed ChIP and semiquantitative PCR assays. Cells were transiently transfected with a vector, Mst1-WT, or the Mst1-T120A mutant construct, followed by 6-h androgen stimulation in serum-starved conditions. Cross-linked protein and DNA complexes were precipitated with anti-AR antibody. Semiquantitative PCR using a primer set spanning the ARE core region of the PSA promoter was performed to determine the abundance of bound DNA in the ChIP complex. The ARE core consists of multiple AREs and plays a crucial role in androgen-mediated PSA promoter activation (21, 30). Fig. 7*D* showed that the Mst1-T120A mutant reduced the androgen induction of AR-chromatin complex formation compared with the vector control, but not the Mst1-WT. These observations suggest that phospho-Thr-120 negatively regulates the formation of inhibitory protein complexes between the AR and Mst1-WT, and that, in turn, most likely leads to the hyperactivation of AR-driven gene expression, leading to cell growth and survival.

DISCUSSION

Mst1 is a part of the evolutionarily conserved RASSF (Ras Associated domain Family) and LATS (Large Tumor Suppressor) protein network (31). The reduction or loss of Mst1 functions by promoter methylation is implicated in the etiology of many cancers (10, 11, 13, 18, 19). Here we described an additional mechanism of Mst1 regulation, facilitated by altered phosphorylation, that is potentially associated with the loss of Mst1 functions in prostate cancer cells. The evidence supporting this conclusion includes the following: 1) phospho-Thr-120, which mainly localized to cell nuclei, might not affect the nuclear localization and cleavage of Mst1; 2) phospho-Mst1-Thr-183 was exclusively found in the cytoplasm; 3) PI3K/Akt and mTOR pathway signaling appeared to differentially and indirectly regulate phospho-Mst1-Thr-120 and phospho-Mst1-T83 in a discrete cell location; 4) phospho-Thr-120 limits the ability of Mst1 to restrict cell growth and survival *ex vivo* as well as tumor growth *in vivo*; and 5) phospho-Thr-120 decreased the Mst1 diminution of AR-driven gene expression. Collectively, these findings indicate that the deregulation of mammalian hippo signaling by aberrant phosphorylation, perhaps in conjunction with altered subcellular localization, provides cell survival and tumor promoting functions. This may have important biologic and therapeutic implications in human prostate cancer.

Mst1 can be deregulated by multiple mechanisms such as promoter methylation (10, 11) and altered subcellular localization with the loss of cytoplasmic expression (13). Cleavage and

nuclear localization are important mechanisms for Mst1 activation and apoptosis. Phospho-Thr-120 was suggested to prevent the nuclear localization and cleavage of Mst1 in ovarian cancer cells (6). Here we found that Mst1-FL, but not the cleaved Mst1-N, localized to the nuclei of prostate cancer cells. Our data indicated that the majority of phospho-Mst1-Thr-120 was accumulated in the nucleus, and that phospho-Thr-120 did not significantly affect the Mst1 nuclear localization and cleavage. In addition, our analysis suggested that total Mst1 and phospho-Mst-Thr-120 protein were mostly found in the cytoplasm of breast or ovarian cancer cells (data not shown). Moreover, phospho-Thr-120 was implicated to prevent phospho-Mst-Thr-183 in ovarian cancer cells (6). We found that phospho-Mst1-Thr-183 was accumulated exclusively in the cytoplasm of prostate tumor cells. In addition, our observations were consistent with the published study (6) showing that the inhibition of PI3K signaling by potent pharmacologic inhibitor LY294002 enhanced cytoplasmic phospho-Mst1-Thr-183. Nevertheless, no change of phospho-Mst1-Thr-183 was observed when cells were treated with a known potent mTOR inhibitor, Ku0063794 or CCI-779. Besides, our IHC data further indicated that the phosphorylation of Mst1 at Thr-120 or Thr-183 occurred concurrently with an increasing expression in prostate tumor samples compared with the non-cancerous counterparts. These findings suggest that the regulation of phospho-Mst1-Thr-120 or phospho-Mst1-Thr-183 is an unrelated event or is modulated by different mechanisms. However, our observations do not rule out the possibility that phospho-Thr-120 could prevent the expression of nuclear phospho-Mst1-Thr-183 in prostate cancer cells. Therefore, we suggest that context-dependent mechanisms might explain the differences between our findings here and findings in the literature (6).

The PI3K/Akt (34) and mTOR (35, 36) oncogenic pathways play a prominent role in the etiology of many cancers (37, 38), including prostate cancer (34). About 30–50% of prostate cancer cases have the hyperactivation of Akt and mTOR signaling because of PTEN loss (39). PI3K/Akt signaling activates mTOR through phosphorylation and inactivation of mTOR negative regulators (40). Because PI3K/Akt and mTOR pathway signaling is central to many cancers, several small molecule inhibitors have been developed to interrogate the PI3K/Akt and mTOR pathways, mainly focusing on mTOR signaling (27, 41–43). These inhibitors are being tested in cell cultures, animal models, or clinical trials as anticancer agents (39). However, success has been very limited (41). Akt is a key component of the PI3K and mTOR pathways (44). Phosphorylation of Akt (referred to Akt1) at the Thr-308 residue by phosphoinositide-dependent kinase 1 (PDK1) (22) and at the Ser-473 residue by mTORC2 leads to the full activation of Akt (32, 40). A negative feedback mechanism as a result of mTOR inhibition was suggested to activate Akt through PI3K signaling (27, 28). We did not observe the up-regulation of phospho-Akt-Ser-473 by mTOR inhibitors in our cell models. Surprisingly, however, we discovered that mTORC1/2 inhibition by Ku0063794 or mTORC1 inhibition by CCI-779 resulted in the up-regulation of phospho-Mst1-Thr-120. This was observed only in the nuclei of castration-resistant C4-2 but not in hormone sensitive LNCaP prostate cancer cells. Our data further demonstrated that a dual inhibition of PI3K and mTOR signaling by BEZ 235 significantly reduced nuclear phospho-Mst1-Thr-120. In addition, we noticed that, as opposed to the phospho-Akt-Ser-473, a considerable amount of nuclear phospho-Akt-Thr-308 was left unaffected by BEZ 235. A similar result was also observed with LY294002. These findings raise the question whether nuclear phospho-Akt-Thr-308 function as a prime kinase for the Thr-120 amino acid residue. This deserves further investigation but is beyond the scope of this study. Overall, our findings suggest that PI3K and mTOR signaling directly or indirectly mediate phospho-Mst1-Thr-120. Moreover, our unpublished data[3] indicated that protein kinase A, protein kinase C, or JNK signaling might also regulate phospho-Mst1-Thr-120 but without having no effect on cytoplasmic phospho-Mst1-Thr-183 (not shown). This suggests that phospho-Mst1-Thr-120 is a target of multiple signaling mechanisms.

In addition, our data indicated that castration-resistant C4-2 cells displayed resistance to the mTOR inhibitor compared with the parental LNCaP line. Consistent with this observation, the induction of a phosphorylation-deficient Mst1-T120A mutant significantly sensitized C4-2 cells to CCI-779 relative to the Mst1-WT or the phosphomimetic Mst1-T120D mutant. Moreover, a published study suggested that Mst1 and Mst2 were functionally redundant and they compensated the absence of each other (29). In light of this observation, one can expect that the viability of C4-2 cells should be reduced significantly by CCI-779 in Mst2 knockdown conditions if Mst1 is functional and able to compensate for the Mst2 absence. Nevertheless, our data showed that C4-2 cells with Mst2 knockdown, but not Mst1, failed to sensitize C4-2 cells to CCI-779. We recognize that the regulation of cell viability by CCI-779 in response to the induction of the Mst1-T120A mutant and/or the reduction of Mst1 expression by RNAi is mechanistically different. Nonetheless, the results from these two independent experiments reinforce and support the notion that phospho-Mst1-Thr-120 might be functionally deregulated.

Finally, our data demonstrated that the Mst1-T120A mutant formed an enhanced protein complex with AR but without altering the AR-chromatin complex formation compared with the Mst1-WT. This suggests that phospho-Thr-120 has a negative impact on the formation of inhibitory protein complexes between the AR and Mst1, supporting the hyperactivation of AR-dependent gene expression whose protein products play a crucial role in cell survival (33), given that the reduction or loss of Mst1 is implicated in a poorer prostate cancer prognosis (18, 19). Thus, deregulation of Mst1 by altered phosphorylation might provide an additional mechanism that potentially contributes to prostate cancer progression and acquired chemoresistance. The model shown in Fig. 7*E* summarizes our findings that signals initiated from or mediated by the PI3K and/or mTOR pathways deregulate Mst1, leading AR hyperactivation and providing cell growth/survival. Nevertheless, future analyses are warranted to explore the mechanisms underlying the molecular interaction between Mst/hippo and mTOR signaling

[3] F. K. Collak and B. Cinar, unpublished data.

and to define whether there may be a functional association between nuclear phospho-Mst1-Thr-120 and disease progression in human cancers.

Acknowledgments—We thank Drs. Leland Chung, Michael Freeman, Neil Bhowmick, Hyung Kim, and Cy Stein for critically evaluating the data; Sandra Orsulic for providing the OVCAR5 ovarian cancer cell line; and Gary Mawyer and Walid Sabbagh for editing the manuscript.

REFERENCES

1. Hay, B. A., and Guo, M. (2003) Coupling cell growth, proliferation, and death. Hippo weighs in. *Dev. Cell* **5,** 361–363
2. Harvey, K. F., Pfleger, C. M., and Hariharan, I. K. (2003) The *Drosophila* Mst ortholog, hippo, restricts growth and cell proliferation and promotes apoptosis. *Cell* **114,** 457–467
3. Creasy, C. L., Ambrose, D. M., and Chernoff, J. (1996) The Ste20-like protein kinase, Mst1, dimerizes and contains an inhibitory domain. *J. Biol. Chem.* **271,** 21049–21053
4. Praskova, M., Khoklatchev, A., Ortiz-Vega, S., and Avruch, J. (2004) Regulation of the MST1 kinase by autophosphorylation, by the growth inhibitory proteins, RASSF1 and NORE1, and by Ras. *Biochem. J.* **381,** 453–462
5. Jang, S. W., Yang, S. J., Srinivasan, S., and Ye, K. (2007) Akt phosphorylates MstI and prevents its proteolytic activation, blocking FOXO3 phosphorylation and nuclear translocation. *J. Biol. Chem.* **282,** 30836–30844
6. Yuan, Z., Kim, D., Shu, S., Wu, J., Guo, J., Xiao, L., Kaneko, S., Coppola, D., and Cheng, J. Q. (2010) Phosphoinositide 3-kinase/Akt inhibits MST1-mediated pro-apoptotic signaling through phosphorylation of threonine 120. *J. Biol. Chem.* **285,** 3815–3824
7. Graves, J. D., Draves, K. E., Gotoh, Y., Krebs, E. G., and Clark, E. A. (2001) Both phosphorylation and caspase-mediated cleavage contribute to regulation of the Ste20-like protein kinase Mst1 during CD95/Fas-induced apoptosis. *J. Biol. Chem.* **276,** 14909–14915
8. Ura, S., Masuyama, N., Graves, J. D., and Gotoh, Y. (2001) Caspase cleavage of MST1 promotes nuclear translocation and chromatin condensation. *Proc. Natl. Acad. Sci. U.S.A.* **98,** 10148–10153
9. de Souza, P. M., and Lindsay, M. A. (2004) Mammalian Sterile20-like kinase 1 and the regulation of apoptosis. *Biochem. Soc. Trans.* **32,** 485–488
10. Steinmann, K., Sandner, A., Schagdarsurengin, U., and Dammann, R. H. (2009) Frequent promoter hypermethylation of tumor-related genes in head and neck squamous cell carcinoma. *Oncol. Rep.* **22,** 1519–1526
11. Seidel, C., Schagdarsurengin, U., Blümke, K., Würl, P., Pfeifer, G. P., Hauptmann, S., Taubert, H., and Dammann, R. (2007) Frequent hypermethylation of MST1 and MST2 in soft tissue sarcoma. *Mol. Carcinog.* **46,** 865–871
12. Qiao, M., Wang, Y., Xu, X., Lu, J., Dong, Y., Tao, W., Stein, J., Stein, G. S., Iglehart, J. D., Shi, Q., and Pardee, A. B. (2010) Mst1 is an interacting protein that mediates PHLPPs' induced apoptosis. *Mol. Cell* **38,** 512–523
13. Minoo, P., Zlobec, I., Baker, K., Tornillo, L., Terracciano, L., Jass, J. R., and Lugli, A. (2007) Prognostic significance of mammalian sterile20-like kinase 1 in colorectal cancer. *Mod. Pathol.* **20,** 331–338
14. Lu, L., Li, Y., Kim, S. M., Bossuyt, W., Liu, P., Qiu, Q., Wang, Y., Halder, G., Finegold, M. J., Lee, J. S., and Johnson, R. L. (2010) Hippo signaling is a potent *in vivo* growth and tumor suppressor pathway in the mammalian liver. *Proc. Natl. Acad. Sci. U.S.A.* **107,** 1437–1442
15. Song, H., Mak, K. K., Topol, L., Yun, K., Hu, J., Garrett, L., Chen, Y., Park, O., Chang, J., Simpson, R. M., Wang, C. Y., Gao, B., Jiang, J., and Yang, Y. (2010) Mammalian Mst1 and Mst2 kinases play essential roles in organ size control and tumor suppression. *Proc. Natl. Acad. Sci. U.S.A.* **107,** 1431–1436
16. Zeng, Q., and Hong, W. (2008) The emerging role of the hippo pathway in cell contact inhibition, organ size control, and cancer development in mammals. *Cancer Cell* **13,** 188–192
17. Zhou, D., Zhang, Y., Wu, H., Barry, E., Yin, Y., Lawrence, E., Dawson, D., Willis, J. E., Markowitz, S. D., Camargo, F. D., and Avruch, J. (2011) Mst1 and Mst2 protein kinases restrain intestinal stem cell proliferation and colonic tumorigenesis by inhibition of Yes-associated protein (Yap) overabundance. *Proc. Natl. Acad. Sci. U.S.A.* **108,** E1312–1320
18. Cinar, B., Fang, P. K., Lutchman, M., Di Vizio, D., Adam, R. M., Pavlova, N., Rubin, M. A., Yelick, P. C., and Freeman, M. R. (2007) The pro-apoptotic kinase Mst1 and its caspase cleavage products are direct inhibitors of Akt1. *EMBO J.* **26,** 4523–4534
19. Cinar, B., Collak, F. K., Lopez, D., Akgul, S., Mukhopadhyay, N. K., Kilicarslan, M., Gioeli, D. G., and Freeman, M. R. (2011) MST1 is a multifunctional caspase-independent inhibitor of androgenic signaling. *Cancer Res.* **71,** 4303–4313
20. Kim, D., Shu, S., Coppola, M. D., Kaneko, S., Yuan, Z. Q., and Cheng, J. Q. (2010) Regulation of proapoptotic mammalian ste20-like kinase MST2 by the IGF1-Akt pathway. *PloS ONE* **5,** e9616
21. Cinar, B., Yeung, F., Konaka, H., Mayo, M. W., Freeman, M. R., Zhau, H. E., and Chung, L. W. (2004) Identification of a negative regulatory cis-element in the enhancer core region of the prostate-specific antigen promoter: implications for intersection of androgen receptor and nuclear factor κB signalling in prostate cancer cells. *Biochem. J.* **379,** 421–431
22. Ding, Z., Liang, J., Li, J., Lu, Y., Ariyaratna, V., Lu, Z., Davies, M. A., Westwick, J. K., and Mills, G. B. (2010) Physical association of PDK1 with AKT1 is sufficient for pathway activation independent of membrane localization and phosphatidylinositol 3 kinase. *PloS ONE* **5,** e9910
23. Carver, B. S., Chapinski, C., Wongvipat, J., Hieronymus, H., Chen, Y., Chandarlapaty, S., Arora, V. K., Le, C., Koutcher, J., Scher, H., Scardino, P. T., Rosen, N., and Sawyers, C. L. (2011) Reciprocal feedback regulation of PI3K and androgen receptor signaling in PTEN-deficient prostate cancer. *Cancer Cell* **19,** 575–586
24. Mulholland, D. J., Tran, L. M., Li, Y., Cai, H., Morim, A., Wang, S., Plaisier, S., Garraway, I. P., Huang, J., Graeber, T. G., and Wu, H. (2011) Cell autonomous role of PTEN in regulating castration-resistant prostate cancer growth. *Cancer Cell* **19,** 792–804
25. Ikenoue, T., Hong, S., and Inoki, K. (2009) Monitoring mammalian target of rapamycin (mTOR) activity. *Methods Enzymol.* **452,** 165–180
26. Zhou, H., Luo, Y., and Huang, S. (2010) Updates of mTOR inhibitors. *Anticancer Agents Med. Chem.* **10,** 571–581
27. Tamburini, J., Chapuis, N., Bardet, V., Park, S., Sujobert, P., Willems, L., Ifrah, N., Dreyfus, F., Mayeux, P., Lacombe, C., and Bouscary, D. (2008) Mammalian target of rapamycin (mTOR) inhibition activates phosphatidylinositol 3-kinase/Akt by up-regulating insulin-like growth factor-1 receptor signaling in acute myeloid leukemia. Rationale for therapeutic inhibition of both pathways. *Blood* **111,** 379–382
28. Yang, S., Xiao, X., Meng, X., and Leslie, K. K. (2011) A mechanism for synergy with combined mTOR and PI3 kinase inhibitors. *PloS ONE* **6,** e26343
29. Oh, S., Lee, D., Kim, T., Kim, T. S., Oh, H. J., Hwang, C. Y., Kong, Y. Y., Kwon, K. S., and Lim, D. S. (2009) Crucial role for Mst1 and Mst2 kinases in early embryonic development of the mouse. *Mol. Cell Biol.* **29,** 6309–6320
30. Cleutjens, K. B., van der Korput, H. A., van Eekelen, C. C., van Rooij, H. C., Faber, P. W., and Trapman, J. (1997) An androgen response element in a far upstream enhancer region is essential for high, androgen-regulated activity of the prostate-specific antigen promoter. *Mol. Endocrinol.* **11,** 148–161
31. Guo, C., Tommasi, S., Liu, L., Yee, J. K., Dammann, R., and Pfeifer, G. P. (2007) RASSF1A is part of a complex similar to the *Drosophila* Hippo/Salvador/Lats tumor-suppressor network. *Curr. Biol.* **17,** 700–705
32. Werzowa, J., Cejka, D., Fuereder, T., Dekrout, B., Thallinger, C., Pehamberger, H., Wacheck, V., and Pratscher, B. (2009) Suppression of mTOR complex 2-dependent AKT phosphorylation in melanoma cells by combined treatment with rapamycin and LY294002. *Br. J. Dermatol.* **160,** 955–964
33. Ghosh, P. M., Malik, S. N., Bedolla, R. G., Wang, Y., Mikhailova, M., Prihoda, T. J., Troyer, D. A., and Kreisberg, J. I. (2005) Signal transduction pathways in androgen-dependent and -independent prostate cancer cell proliferation. *Endocr. Relat. Cancer* **12,** 119–134
34. Deocampo, N. D., Huang, H., and Tindall, D. J. (2003) The role of PTEN in the progression and survival of prostate cancer. *Minerva Endocrinol.* **28,** 145–153

35. Zoncu, R., Efeyan, A., and Sabatini, D. M. (2011) mTOR. From growth signal integration to cancer, diabetes, and ageing. *Nat. Rev. Mol. Cell Biol.* **12,** 21–35
36. Sabatini, D. M. (2006) mTOR and cancer. Insights into a complex relationship. *Nat. Rev. Cancer* **6,** 729–734
37. Liu, P., Cheng, H., Roberts, T. M., and Zhao, J. J. (2009) Targeting the phosphoinositide 3-kinase pathway in cancer. *Nat. Rev. Drug Discov.* **8,** 627–644
38. Liu, Q., Thoreen, C., Wang, J., Sabatini, D., and Gray, N. S. (2009) mTOR-mediated anti-cancer drug discovery. *Drug Discov. Today Ther. Strateg.* **6,** 47–55
39. Morgan, T. M., Koreckij, T. D., and Corey, E. (2009) Targeted therapy for advanced prostate cancer. Inhibition of the PI3K/Akt/mTOR pathway. *Curr. Cancer Drug Targets* **9,** 237–249
40. Zeng, Z., Sarbassov dos, D., Samudio, I. J., Yee, K. W., Munsell, M. F., Ellen Jackson, C., Giles, F. J., Sabatini, D. M., Andreeff, M., and Konopleva, M. (2007) Rapamycin derivatives reduce mTORC2 signaling and inhibit AKT activation in AML. *Blood* **109,** 3509–3512
41. Behbakht, K., Sill, M. W., Darcy, K. M., Rubin, S. C., Mannel, R. S., Waggoner, S., Schilder, R. J., Cai, K. Q., Godwin, A. K., and Alpaugh, R. K. (2011) Phase II trial of the mTOR inhibitor, temsirolimus and evaluation of circulating tumor cells and tumor biomarkers in persistent and recurrent epithelial ovarian and primary peritoneal malignancies. A Gynecologic Oncology Group study. *Gynecol. Oncol.* **123,** 19–26
42. Bhagwat, S. V., and Crew, A. P. (2010) Novel inhibitors of mTORC1 and mTORC2. *Curr. Opin. Investig. Drugs* **11,** 638–645
43. Meric-Bernstam, F., and Gonzalez-Angulo, A. M. (2009) Targeting the mTOR signaling network for cancer therapy. *J. Clinic. Oncol.* **27,** 2278–2287
44. Fayard, E., Xue, G., Parcellier, A., Bozulic, L., and Hemmings, B. A. (2010) Protein kinase B (PKB/Akt), a key mediator of the PI3K signaling pathway. *Curr. Top. Microbiol. Immunol.* **346,** 31–56